Creating number states in the micromaser using feedback

Ariel Liebman and G.J. Milburn
Physics Department, University of Queensland, St. Lucia, 4072, Brisbane, Australia
(Received 12 May 1994)

We use the quantum theory of feedback developed by Wiseman and Milburn [Phys. Rev. Lett. **70**, 548 (1993)] and Wiseman [Phys. Rev. A **49**, 2133 (1994)] to investigate the photon-number noise properties of the micromaser with direct detection feedback. We find that the feedback can significantly reduce the amount of noise in the photon number. Under the right conditions the feedback locks the system onto a number state. As opposed to other schemes in the past [P. Meystre, Opt. Lett. **12**, 669 (1987); J. Krause, M.O. Scully, and H. Walther, Phys. Rev. A **36**, 4547 (1987)], we can fix the number state to which the system evolves. We also simulate the micromaser using the quantum-trajectories method and show that these results agree with the quantum theory of feedback. We show that the noise of quantum island states [P. Bogar, J.A. Bergou, and M. Hillary, Phys. Rev. A **50**, 754 (1994)] can be significantly reduced by the feedback.

PACS number(s): 42.50.Ar, 42.50.Dv, 42.52.+x

I. INTRODUCTION

In recent years, there has been a great deal of experimental progress in the field of cavity QED and quantum optics [1,3,2]. The development of a superconducting cavity in the microwave regime is particularly notable since it has enabled very large Q factors to be achieved. This enables the strong coupling regime to be realized [3], where the strength of the interaction g is much greater than the cavity damping and the transverse spontaneous emission rates. The microwave cavity is made of pure Niobium and cooled down to a fraction of a kelvin. Quality factors of up to 3×10^{10} can thus be reached. These cavities have exceedingly small losses and can be thought of as "photon traps" for relatively long time scales.

Since the atomic transition is only resonant with one of the cavity modes the dynamics of the system exhibit a nearly periodic exchange of energy between the atom and the cavity mode, that is, Rabi oscillations.

In the microscopic maser or micromaser, the atoms are injected into the cavity at a low rate r such that only one atom at a time is present in the cavity. This requires that the mean time between atoms, r^{-1}, is much greater than then transit time through the cavity τ. The transit time of the atoms can be controlled by a Fizeau velocity selector [2].

The micromaser can be operated in a regime where spontaneous emission into modes other than the cavity mode can be neglected and the photon lifetime γ_c^{-1} is very long compared with the atomic transit time τ. Hence, we can neglect the decay of the cavity during the interaction time of the atom with the field. The interaction between the atom and the field can then be described by a kick superoperator. Using the language of operators and effects we can, therefore, elegantly derive a master equation for the cavity mode. The language of operations and effects to be discussed in Sec. II will be used throughout this paper.

As there are no good detectors of light in the microwave region the only way to measure the state of the field is to detect the state of the atoms exiting the cavity. Let all atoms enter the cavity in the excited state. Then the probability of an atom leaving in the lower state is related to the photon-number inside the cavity through the relation

$$P_g = r \left\langle \sin(\mu\sqrt{a^\dagger a + 1}) \right\rangle , \tag{1.1}$$

where $\mu = g\tau$ is the scaled interaction strength. This suggests that we can use this information to modify some parameter of the system through a feedback mechanism. The most obvious choice is the damping rate of the cavity. The reasoning here is that an increase in the detection rate of atoms leaving in the ground state must in some way indicate that the photon number inside the cavity has changed. We then increase the damping rate by a small amount. In other words, we assume that on average a higher atomic count rate indicates a higher photon number in some circumstances (depending on the photon-number distribution and the value of the pumping parameter $g\tau$). Figure 1 shows a diagram of the system model.

In this paper, we perform this calculation using two different methods. In Sec. VII we use the Markovian quantum feedback theory developed by Wiseman [4], and we present the results of quantum-trajectories simulations of the micromaser with feedback in Sec. X. It should be noted the quantum feedback theory also has its origins in the quantum-trajectories method.

Our results show that the feedback can enhance the sub-Poissonian characteristics of the micromaser when the damping is very small compared with the driving rate. For significant damping rates, the feedback degrades the photon-number squeezing in the micromaser in the usual regimes described in the literature [5]. We also show that there are regimes where even for significant damping the squeezing is enhanced. In the small damping case, we can form a state very close to a num-

1050-2947/95/51(1)/736(16)/$06.00 ©1995 The American Physical Society

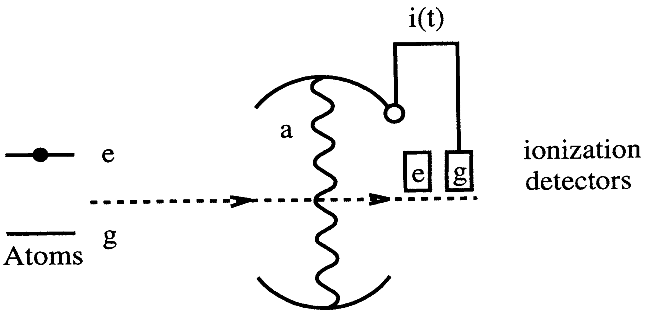

FIG. 1. The feedback scheme where the ionization detection current is fed back onto the damping rate of the cavity.

ber state. This state is determined by the strength of the feedback used and is a great improvement on other schemes to generate number states where the final number state is unpredictable [6].

II. THE LANGUAGE OF OPERATORS AND EFFECTS

The most convenient quantum description of measurement, for our purposes, is provided by the formalism of operations and effects [7]. This is an extension of the usual projection postulate to account for more realistic measurement schemes. In the standard presentation, a measurement of a quantity represented by an operator $\hat{A}$, with eigenvalues a, gives a result a with probability $P(a) = \mathrm{Tr}(\rho|a\rangle\langle a|)$, where ρ is the state of the system prior to measurement. The conditional state of the system based on this result, is given by $|a\rangle\langle a|$. No real measurements can be described in this way, as there is always some additional statistical error in the measurement result. Indeed in some cases, demolition photon counting for example, the conditional state is nothing like a diagonal projector.

We generalize the projection approach as follows. The probability of obtaining the result a is given in terms of a positive operator $\hat{F}(a)$ by

$$P(a) = \mathrm{Tr}[\rho\hat{F}(a)] \ , \tag{2.1}$$

where, for normalization, we require that $\sum_a \hat{F}(a) = \hat{1}$. The conditional state of the system, conditioned on this result is given by

$$\rho^{(a)} = [P(a)]^{-1}\,\phi_a\rho \ , \tag{2.2}$$

where ϕ_a acts on the space of density operators and is called an operation. Clearly, $\mathrm{Tr}[\rho\hat{F}(a)] = \mathrm{Tr}[\phi_a\rho]$. The unconditioned state of the system after the measurement is given by

$$\rho' = \sum_a P(a)\rho^{(a)} = \sum_a \phi_a\rho \ . \tag{2.3}$$

It can be shown [8] that the most general operation can be written in the form

$$\Phi\rho = \sum_j A_j\rho A_j^\dagger \ , \tag{2.4}$$

where each $A_j^\dagger A_j$ is a positive operator.

As an example, we consider photon counting from a cavity mode. If all photons lost from the cavity are counted with unit efficiency, the rate of counting is given by $\gamma\mathrm{Tr}(a^\dagger a\rho)$, where $a, a^\dagger$ are the cavity mode annihilation and creation operators and γ is the loss rate from the cavity. The unnormalized conditional state of the cavity given one count between t and $t + dt$ is

$$\tilde{\rho}^{(1)}(t+dt) = \mathcal{J}\rho(t)dt \tag{2.5}$$

$$= \gamma a\rho a^\dagger dt \ . \tag{2.6}$$

The probability of this event is given by $\mathrm{Tr}[\mathcal{J}\rho(t)] = \gamma\mathrm{Tr}[a^\dagger a\rho(t)]dt$.

III. THE JAYNES-CUMMINGS MODEL

The simplest model for the interaction between a two level atom and a single mode field on resonance was given by Jaynes and Cummings [9]. The Hamiltonian is commonly known as the Jaynes-Cummings Hamiltonian and is given by

$$H = \frac{1}{2}\hbar\omega\sigma_z + \hbar\omega a^\dagger a + \hbar g\left(a^\dagger\sigma^- + a\sigma^+\right) . \tag{3.1}$$

The coupling coefficient g is related to the electric-dipole matrix element through

$$g = \langle e|\,\hat{D}\,|g\rangle\,\mathcal{E}_0/\hbar, \tag{3.2}$$

where $\mathcal{E}_0$ is the field per photon in a cavity with an effective mode volume V given by

$$\mathcal{E}_0 = (\hbar\omega/2\epsilon_0 V)^{1/2}, \tag{3.3}$$

and $\hat{D}$ is the electric-dipole-moment operator. The state of the field after the interaction with an atom for a time τ is given by

$$\rho_f(t+\tau) = \phi_\tau(\rho(t)) = \mathrm{Tr}_a\left[U(\tau)\rho_a\otimes\rho_f U^\dagger(\tau)\right] , \tag{3.4}$$

where

$$U(\tau) = e^{-i\tau\left(ga^\dagger\sigma^- + g^*a\sigma^+\right)}, \tag{3.5}$$

and ρ is the field density matrix. Note that there is an implicit assumption in using the trace that nonselective measurement has occurred. We know an atom has left the cavity but we do not know in which state. If the atom enters in an incoherent mixture of the excited and ground states $(\rho(t)) = \lambda_1|g\rangle\langle g| + \lambda_2|e\rangle\langle e|)$, then the density operator after the interaction is

$$\begin{aligned}\rho(t+\tau) = \phi_\tau(\rho(t)) = {} & \lambda_1\cos(\mu\sqrt{a^\dagger a})\rho\cos(\mu\sqrt{a^\dagger a}) + \lambda_2\cos(\mu\sqrt{aa^\dagger})\rho\cos(\mu\sqrt{aa^\dagger}) \\ & +\lambda_1 a(a^\dagger a)^{-1/2}\sin(\mu\sqrt{a^\dagger a})\rho\sin(\mu\sqrt{a^\dagger a})(a^\dagger a)^{-1/2}a^\dagger \\ & +\lambda_2 a^\dagger(aa^\dagger)^{-1/2}\sin(\mu\sqrt{aa^\dagger})\rho\sin(\mu\sqrt{aa^\dagger})(aa^\dagger)^{-1/2}a,\end{aligned} \tag{3.6}$$

where $\mu = g\tau$. This is the full kick operator with a mixture of excited and ground state atoms passing through the cavity.

IV. THE MASTER EQUATION

As the sequence of times at which the atoms enter the cavity is a Poissonian process, all we need to know is the rate at which the atoms are injected. Let this rate be denoted r. Then the probability of one kick (an injected atom) occurring in an infinitesimally short time Δt is simply $r\Delta t$. If we ignore the damping of the cavity for the duration of the kick, then we can write the new state of the density operator in the case of a kick as

$$\tilde{\rho}(t+\Delta t) = re^{-iH_0/\hbar\Delta t}\phi_\tau(\rho(t))e^{iH_0/\hbar\Delta t}\Delta t, \qquad (4.1)$$

where ϕ_τ was defined by Eq. (3.4) Note that $\text{Tr}[\rho(t+\Delta t)] = r\Delta t$ as the transformation generating the superoperator ϕ_τ is unitary. Thus, the probability of a kick is simply given by $r\Delta t$ and is independent of the actual kick mechanism.

If we begin with an ensemble of identical systems and then choose only those which received a kick, then the new normalized density operator describing this ensemble is given by the selective operation [10]

$$\rho \rightarrow \rho_{\text{new}} = \frac{re^{-iH_0/\hbar\Delta t}\phi_\tau(\rho(t))e^{iH_0/\hbar\Delta t}\Delta t}{\text{Tr}\left[re^{-iH_0/\hbar\Delta t}\phi_\tau(\rho(t))e^{iH_0/\hbar\Delta t}\Delta t\right]}. \qquad (4.2)$$

The complementary operation to the kick is, of course, the no kick interaction which can be denoted by $\tilde{\phi}_\tau$ and occurs with probability $1 - r\Delta t$. If we do not look to see if a kick has occurred, we have a nonselective operation after which the density operator becomes a weighted mean of the kick and no kick results:

$$\rho(t+\Delta t) = r\Delta t e^{-iH_0/\hbar\Delta t}\phi_\tau(\rho(t))e^{iH_0/\hbar\Delta t} + (1 - r\Delta t)\tilde{\phi}_\tau(\rho(t)). \qquad (4.3)$$

It can clearly be seen that the no kick operation is simply given by the free evolution of the system

$$\tilde{\phi}_\tau(\rho(t)) = e^{-iH_0/\hbar\Delta t}\rho(t)e^{iH_0/\hbar\Delta t}. \qquad (4.4)$$

The evolution equation for the density operator under the interaction with the injected atoms can be defined by

$$\frac{d\rho(t)}{dt} = \lim_{\Delta t\rightarrow 0}\frac{\rho(t+\Delta t) - \rho(t)}{\Delta t}. \qquad (4.5)$$

Substituting Eq. (4.3) into the above equation and ignoring all terms of order Δt^2 or higher, we get the following equation

$$\frac{d\rho(t)}{dt} = r[\phi_\tau(\rho(t)) - \rho(t)]. \qquad (4.6)$$

Note that the effect of the free evolution after the kick was ignored because it is of order Δt^2. This master equation was previously obtained in [10].

V. THE ATOMIC MEASUREMENT

In order to know what has happened during the interaction, we need to know whether the atom left in the excited or ground state. This can be done using an ionization detector and first ionizing the atom from the upper state and then from the lower state. Given the result of the measurement, we can obtain the conditional density operator for the field. The new information is used to update the description of the field. If we assume all the atoms are injected in the upper state, then the operations for an atom leaving in the excited and ground states, respectively, are

$$\begin{aligned}\mathcal{J}'(\rho) &= Tr_a\left[|e\rangle\langle e|\,U\rho_a\otimes\rho\,U^\dagger\right] \\ &= \cos\left(g\tau\sqrt{aa^\dagger}\right)\rho\cos\left(g\tau\sqrt{aa^\dagger}\right)\ , \\ \mathcal{J}(\rho) &= Tr_a\left[|g\rangle\langle g|\,U\rho_a\otimes\rho\,U^\dagger\right] \\ &= a\frac{1}{\sqrt{aa^\dagger}}\sin\left(g\tau\sqrt{aa^\dagger}\right)\rho\sin\left(g\tau\sqrt{aa^\dagger}\right)\frac{1}{\sqrt{aa^\dagger}}a^\dagger,\end{aligned} \qquad (5.1)$$

where we have dropped the subscript on the field density matrix for convenience.

If the atoms pass through the cavity at a rate r, then the probability there was an atom in the cavity in any infinitesimal time interval dt is given by $\text{Tr}\left[r(\mathcal{J}'+\mathcal{J})\rho dt\right] = \text{Tr}\left[r\phi_\tau(\rho)dt\right] = rdt$. Then the probability that the atom leaves in the excited or ground states given it entered in the excited state is

$$\begin{aligned}P_e &= \text{Tr}\left[\mathcal{J}'(\rho)\right] = \left\langle\cos^2\left(g\tau\sqrt{aa^\dagger}\right)\right\rangle , \\ P_g &= \text{Tr}\left[\mathcal{J}(\rho)\right] = \left\langle\sin^2\left(g\tau\sqrt{aa^\dagger}\right)\right\rangle ,\end{aligned} \qquad (5.2)$$

respectively.

Note that even if the intracavity field is in a vacuum state the transition probability to the ground state is nonzero. This is simply spontaneous emission into the cavity mode.

VI. QUANTUM TRAJECTORIES AND FEEDBACK

The recently introduced numerical method of stochastic quantum trajectories [11] essentially involves a Monte Carlo style simulation of a physical system described by a master equation of the form of Eq. (6.17). The solutions of equations of this form can be obtained by splitting the equation into two parts:

$$\dot{\rho}(t) = \mathcal{J}\rho + \mathcal{L}_0\rho\ , \qquad (6.1)$$

and writing down the Dyson expansion

$$\rho(t) = \sum_{m=0}^{\infty}\int_0^t dt_m\int_0^{t_m}dt_{m-1}\cdots\int_0^{t_2}dt_1\mathcal{S}_{t-t_m} \times\mathcal{J}\mathcal{S}_{t_m-t_{m-1}}\cdots\mathcal{J}\mathcal{S}_{t_1}\rho(0), \qquad (6.2)$$

where $\mathcal{J}$ is a jump superoperator denoting some form of measurement and $\mathcal{S}$ is a smooth evolution operator describing the zero count part of the evolution. In the case of a damped harmonic oscillator this operator will be

$$\mathcal{S}_t\rho = e^{\left(\frac{-i}{\hbar}H_0 - \frac{\gamma}{2}a^\dagger a\right)t}\rho(0)e^{\left(\frac{i}{\hbar}H_0 - \frac{\gamma}{2}a^\dagger a\right)t}, \quad (6.3)$$

and $\mathcal{J}$ is as defined in Eq. (2.6). The Hermitian Hamiltonian part of the superoperator describes the unitary reversible evolution of the system. The non-Hermitian part describes the irreversible decay of the probability, which can be thought of as being a consequence of our gaining more information about the system. That is, the longer we wait for a count the more certain it is that the photon number in the cavity is lower than it was thought.

It was asserted by Carmichael that one can obtain a solution to the master equation by calculating a large number of possible realizations of the sequence of counts described by

$$\rho_c(t) = \mathcal{S}_{t-t_m}\mathcal{J}\mathcal{S}_{t_m-t_{m-1}}\cdots\mathcal{J}\mathcal{S}_{t_1}\rho(0), \quad (6.4)$$

where the subscript c on the density operator denotes that the result is conditioned on a certain sequence of m counts at times $(t_m, t_{m-1}, \ldots, t_1)$. In other words, this sequence of operations describes the selective evolution of the density operator. Note that this density operator is unnormalized and, thus, the probability of a particular sequence of counts occurring at particular times $(t_m, t_{m-1}, \ldots, t_1)$ is simply the trace of the conditioned density operator,

$$\begin{aligned} P(\rho_c(t)) &= \mathrm{Tr}[\rho_c(t)] \\ &= \mathrm{Tr}\left[\mathcal{S}_{t-t_m}\mathcal{J}\mathcal{S}_{t_m-t_{m-1}}\cdots\mathcal{J}\mathcal{S}_{t_1}\rho(0)\right]. \end{aligned} \quad (6.5)$$

The overall solution of the master equation is simply the ensemble average of the resulting density matrices. That is,

$$\begin{aligned} \rho(t) &= \sum_R \frac{\rho_c(t)}{P(\rho_c(t))}P(\rho_c(t)) \\ &= \sum_R \mathcal{S}_{t-t_m}\mathcal{J}\mathcal{S}_{t_m-t_{m-1}}\cdots\mathcal{J}\mathcal{S}_{t_1}\rho(0), \end{aligned} \quad (6.6)$$

where R denotes all possible realizations of a counting process including time ordered integrals over the count times. This is known as the nonselective evolution of the system. The numerical technique for using this method in calculating the solution to the micromaser will be presented in Sec. X.

The formalism of the quantum trajectories was applied by Wiseman and Milburn to feedback with homodyne detection [12] and later generalized to all discrete detection processes such as photon counting [4].

Quantum feedback

The quantum-mechanical model of a real physical feedback process can be approached from a quantum measurement point of view, an alternative method is to take the all optical approach using quantum Langevin equations. In the case of the micromaser, where the quantum Langevin [13] approach would be quite complicated, we prefer to use the measurement-theory method where the feedback, as it is manifested in the master equation, is more transparent. In this section, we will describe the general principles behind the Wiseman model of feedback and apply it to the micromaser.

The detection process in the case of the micromaser, where the detection occurs via the state of the atoms, is a point process. That is to say, the counts are a sequence of δ-function events interspersed with long periods of free evolution of the system. In the case of a micromaser with Poissonian pumping, the count process for detecting atoms in the ground or excited states is also Poissonian. For example, the probability of detecting an atom in the ground state is simply $P_g = r\,\mathrm{Tr}[\mathcal{J}\rho]dt$.

It is useful to denote a Poissonian count processes through a random increment, which we will call $dN_c(t)$. By "increment" we mean the change in the atomic count number in an infinitesimal interval dt. This interval is short enough so that the count total is only ever increased by 1. Thus, dN_c is a random variable which takes on the values of 0 or 1. The probability of getting a count in an interval dt is much less than 1. The increment has a subscript c on it to remind ourselves that this counting sequence is related to the conditional evolution of the system, that is, it depends on the previous history of the counts.

As an example of a Poissonian process, we present the familiar case of a simple photon-counting process. Since the increment can only take on the values 0 or 1 the following two conditions hold, and in fact, define the Poissonian-counting process. The conditions then are

$$\begin{aligned} dN_c(t)^2 &= dN_c(t)\ , \\ E[dN_c(t)] &= \kappa dt\,\mathrm{Tr}[a\rho_c(t)a^\dagger]. \end{aligned} \quad (6.7)$$

Consequently, the conditional evolution equation is [14]

$$\begin{aligned} d\rho_c(t) = dN_c(t)&\left[\frac{\mathcal{J}\rho_c(t)}{\langle n\rangle_c(t)} - \rho_c(t)\right] \\ &+dt\left(\langle n\rangle_c(t)\rho_c(t) - \frac{1}{2}\left[n\rho_c(t) + \rho_c(t)n\right]\right. \\ &\left.-\frac{i}{\hbar}\left[\rho_c(t), H_0\right]\right), \end{aligned} \quad (6.8)$$

where $n = a^\dagger a$. When an expectation over the variable dN is taken, this equation reduces to the standard damped oscillator master equation.

One might think we could also write down a similar stochastic equation for the micromaser with the detection of an atom in the ground state only using a random process defined by

$$\begin{aligned} dN_c(t)^2 &= dN_c(t)\ , \\ E[dN_c(t)] &= \mathrm{Tr}[r\mathcal{J}\rho_c(t)dt] = rdt\mathrm{Tr}[\phi_g\rho_c(t)]. \end{aligned} \quad (6.9)$$

However, the random process $dN_c(t)$ is, in fact, a combination of two processes, the injection of an atom and then the transition of an atom to the ground state. Let these processes be dA, the process for the injection of an atom, and the conditional process M, which denotes whether the atom has made a transition to the ground state ($M = 1$). These obey the following rules:

$$\begin{aligned} dA_c(t)^2 &= dA_c(t)\ , \\ E[dA_c(t)] &= rdt\ , \\ M_c(t)^2 &= M_c(t)\ , \\ E[M_c(t)] &= \left\langle \sin^2(\mu\sqrt{aa^\dagger}) \right\rangle . \end{aligned} \tag{6.10}$$

The full conditional equation is then

$$\begin{aligned} d\rho_c(t) = {} & dA_c(t)M_c(t)\left[\frac{\mathcal{J}\rho_c(t)}{\mathrm{Tr}[\mathcal{J}\rho_c(t)]} - \rho_c(t)\right] \\ & + dA_c(t)[1 - M_c(t)]\left[\frac{\mathcal{J}'\rho_c(t)}{\mathrm{Tr}\left[\mathcal{J}'\rho_c(t)\right]} - \rho_c(t)\right] . \end{aligned} \tag{6.11}$$

Again, this reduces to the micromaser-master equation when an expectation value is taken.

Now we can introduce feedback into the system by using the method developed by Wiseman [4]. He defined the feedback through the master equation,

$$\dot{\rho}_c(t) = \frac{dN_c(t-\tau)}{dt}\mathcal{K}\rho_c(t), \tag{6.12}$$

where the strength of the feedback at time t is proportional to the detection current $dN_c(t-\tau)/dt$ at an earlier time. The difficulty in applying this is the fact that the detection current is singular at the times of the detections. This means that we have to calculate the increment in ρ and take the ensemble average before dividing by dt. Wiseman also showed that the effect of the feedback must be applied after the conditional evolution increment in the following way:

$$\begin{aligned} \rho_c(t + dt) = {} & e^{dA_c(t-\tau)M(t-\tau)\mathcal{K}} \\ & \times \left\{ \rho_c(t) + dA_c(t)M_c(t)\left(\frac{\mathcal{J}\rho_c(t)}{\mathrm{Tr}\mathcal{J}\rho_c(t)} - \rho_c(t)\right) \right. \\ & \left. + \, dA_c(t)[1 - M_c(t)]\left(\frac{\mathcal{J}'\rho_c(t)}{\mathrm{Tr}\mathcal{J}'\rho_c(t)} - \rho_c(t)\right) \right\} . \end{aligned} \tag{6.13}$$

The exponential in the above equation is the formal solution to Eq. (6.12) over a time dt. Since we eventually take the infinitesimal limit for dt, the feedback can be thought of as a δ-function kick. This is because the exponent can be written as

$$dA_c(t)M_c(t)\mathcal{K} = \frac{dA_c(t)M_c(t)}{dt}dt\,\mathcal{K} = dt dA_c(t)M_c(t)\frac{1}{dt}\mathcal{K}, \tag{6.14}$$

which means that a feedback of strength $1/dt$ is applied for a time dt. We can expand the exponential and then rewrite it as

$$1 + dA_c(t-\tau)M(t-\tau)\left(e^{\mathcal{K}} - 1\right) . \tag{6.15}$$

Using this and noting that $M(1-M) = 0$ and $E[1-M] = \left\langle \cos^2(\mu\sqrt{aa^\dagger}) \right\rangle$, we get the nonselective feedback master equation by taking the expectation value over the count process,

$$\dot{\rho}(t) = \mathcal{J}\rho(t) + \mathcal{J}'\rho(t) - \rho(t) + \left(e^{\mathcal{K}} - 1\right)\mathcal{J}\rho(t). \tag{6.16}$$

The general form of the operator $\mathcal{K}$ that can be used is

$$\mathcal{K}(\rho) = \frac{-i}{\hbar}\left[\rho, H_0\right] + \mathcal{D}(\rho), \tag{6.17}$$

where the first term is simply the Hamiltonian evolution and the second term is the irreversible evolution. Overall this is said to be of the Lindblad form [15] if

$$\mathcal{D}(\rho) = \sum_j 2A_j\rho A_j^\dagger - A_j^\dagger A_j\rho - \rho A_j^\dagger A_j, \tag{6.18}$$

where again, $A_j^\dagger A_j$ is a positive operator.

Here, we will feed back onto the damping rate of the cavity and, thus, we take the feedback superoperator to be

$$\begin{aligned} \mathcal{K}\rho = \lambda & \left[(1 + n_b)\left(2a\rho a^\dagger - a^\dagger a\rho - \rho a^\dagger a\right)\right. \\ & \left. + \, n_b\left(2a^\dagger\rho a - aa^\dagger\rho - \rho aa^\dagger\right)\right] , \end{aligned} \tag{6.19}$$

where λ is the feedback strength and n_b is the bath parameter. Then assuming that λ is small, we truncate the exponential to second order. It is shown in Sec. X that this master equation method agrees quite well with the quantum-trajectories simulation approach.

VII. THE FEEDBACK MASTER EQUATION

In the interval between atoms, the damping of the field through its interaction with a bath is described by the master equation,

$$\begin{aligned} \dot{\rho_d} = {} & \frac{\kappa}{2}(1 + n_b)\left(2a\rho a^\dagger - a^\dagger a\rho - \rho a^\dagger a\right) \\ & + \frac{\kappa}{2}n_b\left(2a^\dagger\rho a - aa^\dagger\rho - \rho aa^\dagger\right) , \end{aligned} \tag{7.1}$$

where κ is the damping rate of the cavity and n_b is the mean photon number of the bath where the bath is in a thermal state.

Putting all the dynamics of the micromaser together, we get the overall master equation

$$\begin{aligned} \dot{\rho}(t) = {} & \gamma\left[\mathcal{J}\rho(t) + \mathcal{J}'\rho(t) - \rho(t)\right] \\ & + \dot{\rho}_d(t) + \mathcal{K}(\mathcal{J}\rho(t)) + \frac{\mathcal{K}^2}{2}(\mathcal{J}\rho(t)). \end{aligned} \tag{7.2}$$

We truncated the feedback exponential after second order on the assumption that the feedback is small enough. The first three terms describe the normal evolution of the micromaser with all the atoms entering in the excited state ($\lambda_2 = 1$). The fourth term describes the standard cavity damping. The fifth and sixth terms described the feedback drift and diffusion terms. The diffusion term can be thought of as the measurement noise fed back onto the system. This is approximately true in the small feedback limit. This is similar to the master equation derived by Wiseman and Milburn for the case of feedback using a signal from a homodyne detection process. Another similar master equation has been derived by Caves and Milburn [16] in the analysis of the feedback from a continuous measurement process on a kicked system. If λ approaches 1 then the truncation fails and the full exponential must be used.

A. The simple-amplifier limit

If we let the interaction parameter $\mu = g\tau$ be very small so that we can approximate the sine term in $\mathcal{J}$ by its argument,

$$\sin(\mu\sqrt{aa^\dagger}) \approx \mu\sqrt{aa^\dagger}, \tag{7.3}$$

then we can derive a simple-amplifier master equation for the micromaser. In this case, we also approximate $\cos(\mu\sqrt{aa^\dagger})$ by $(1-\mu^2 aa^\dagger/2)$. The master equation then becomes

$$\begin{aligned}\dot{\rho} = {} & r\frac{\mu^2}{2}\left(2a^\dagger\rho a - aa^\dagger\rho - \rho aa^\dagger\right)\\ & +\frac{\kappa}{2}(1+n_b)\left(2a\rho a^\dagger - a^\dagger a\rho - \rho a^\dagger a\right)\\ & +\frac{\kappa}{2}n_b\left(2a^\dagger\rho a - aa^\dagger\rho - \rho aa^\dagger\right)\\ & +\mathcal{K}(r\mu^2 a^\dagger\rho a) + \frac{\mathcal{K}^2}{2}(r\mu^2 a^\dagger\rho a),\end{aligned} \tag{7.4}$$

where we have assumed that the bath is at zero temperature for the sake of simplicity. This approximation essentially means that there is no realistically attainable intracavity photon number for which the evolution of the atom can even remotely approach a full Rabi cycle. That is, the pumping of the maser is linear. We can then take the diagonal elements of this equation to get the following equation for the photon-number distribution in the cavity:

$$\begin{aligned}\dot{p}(n) = {} & r\mu^2\left[np(n-1)-(n+1)p(n)\right] + \kappa\left[(n+1)p(n+1)-np(n)\right] + r\mu^2\lambda\left[(n+1)^2p(n)-n^2p(n-1)\right]\\ & + r\mu^2\frac{\lambda^2}{2}\left[(n+2)^2(n+1)p(n+1)-(n+1)^3p(n)-(n+1)^2np(n)+n^3p(n-1)\right].\end{aligned} \tag{7.5}$$

Solving this equation in the steady state, we can get the following recursion relation for the photon-number distribution $p(n)$:

$$q(n) \equiv \frac{p(n)}{p(n-1)} = r\mu^2\frac{1-\lambda n+\lambda^2n^2/2}{\kappa + r\mu^2\lambda^2/2(n+1)^2}. \tag{7.6}$$

Using the method of Görtz and Walls [17] we will assume that the distribution is single peaked. Then the peak must occur near $p(n) = p(n-1)$. This leads to the requirement that

$$q(n) = r\mu^2\frac{1-\lambda n+\lambda^2n^2/2}{\kappa + r\mu^2\lambda^2/2(n+1)^2} = 1. \tag{7.7}$$

This can be solved in the limit that $\lambda \ll 1$ and assuming that in the presence of feedback we can ignore damping in a good cavity. This is valid if $r \gg \kappa$, the pumping rate is much greater than the damping. The steady-state mean is then

$$\bar{n} = \frac{1}{\lambda}, \tag{7.8}$$

so that the mean photon number is quite large. We can find the variance using the relation

$$V = -\left(\left.\frac{dq}{dn}\right|_{n=\bar{n}}\right)^{-1}. \tag{7.9}$$

This gives

$$V_{ss} = \frac{\bar{n}}{2}. \tag{7.10}$$

Note that the variance is half that of a Poissonian distribution.

B. Time-dependent analysis

We can obtain some time-dependent results using a short time Fokker-Planck analysis. For this purpose, we assume that the distribution starts as a δ-function at some photon number m. This approximate distribution will be denoted by $P(n,t)$. We expand $P(n,t)$ to first order about the initial δ-function. That is, we write

$$P(n,t) = \delta(n-m) + t\,\mathcal{L}P(n,0)|_{P(n,0)=\delta(n-m)}, \tag{7.11}$$

where $\mathcal{L}P(n,t)$ is the right hand side of Eq. (7.5). To find the drift $(a(m))$ and diffusion $(D(m))$ coefficients for the Fokker-Planck equation, we find the first and second order moments from the short time solution above. Hence,

$$ta(m) = t\langle n-m\rangle, \tag{7.12}$$

$$tD(m) = t\left\langle (n-m)^2\right\rangle. \tag{7.13}$$

The corresponding Fokker-Planck equation is

$$\dot{P}(n,t) = \left[-\frac{\partial}{\partial n}a(n) + \frac{1}{2}\frac{\partial^2}{\partial n^2}D(n)\right]P(n,t). \tag{7.14}$$

The Fokker-Planck approximation to the discrete master equation holds if the function $P(n,t)$ varies slowly enough with n.

This Fokker-Planck equation can then be approximated by an Ornstein-Uhlenbeck process about the mean photon number $\bar{n}$. The drift coefficient can be expanded to first order about the mean photon number as

$$a(n) = a(\bar{n}) + a'(\bar{n})(n-\bar{n}). \tag{7.15}$$

The constant drift term can be set to zero around the mean photon number, as we expect there to be no significant drift at that point. This gives us the mean photon number,

$$\bar{n} = \frac{G-\kappa}{\lambda G}, \tag{7.16}$$

which reduces to $1/\lambda$, as before, in the limit of small damping $\kappa \ll r\mu^2$. The other coefficients are

$$k = G - \kappa\ , \tag{7.17}$$

$$D(\bar{n}) = (2\kappa + \lambda^2 G \bar{n}^2)\bar{n}. \tag{7.18}$$

The Fokker-Planck equation is then

$$\dot{P}(x,t) = \left[k\frac{\partial}{\partial x} + \frac{1}{2}D(\bar{n})\frac{\partial^2}{\partial x^2}\right]P(x,t), \tag{7.19}$$

where $k = -a'(\bar{n})$ and $x = n - \bar{n}$ is the deviation from the mean.

The variance in $x(t)$ which is equal to the variance in $n(t)$ is given by [18]

$$V(t) = \frac{D}{2k}(1-e^{-2kt}), \tag{7.20}$$

which reduces to $\bar{n}/2$ at steady state in the limit of small damping.

The steady-state two-time correlation function for the photon-number deviation inside the cavity can also be found using this method to be

$$\langle x(\tau)x(0)\rangle_{ss} = \frac{D}{2k}e^{-k\tau} \approx \frac{\bar{n}}{2}e^{-r\mu^2\tau}. \tag{7.21}$$

VIII. THE FULL MODEL

The more physically interesting regime which occurs for larger values of μ requires the use of the full trigonometric functions in the master equation. It is essential to include these functions in order to study how the trapping states [10] participate in the action of the feedback. A trapping state occurs when the photon number inside the cavity is such that the atom undergoes an integral number of Rabi half cycles. That is, the probability of a transition to the ground state is zero. This occurs for photon numbers n, such that $\mu(n+1)^2 = m\pi$, where m is some integer. This can lead to a single or a comb of number states forming in a lossless micromaser. Especially important is the absence of thermal noise which leads to significant jumping of the probability through the trapping states.

The full master equation in the photon-number basis is

$$\begin{aligned}
\dot{p}(n) = {} & r\left[\sin^2(\mu\sqrt{n})p(n-1) - \sin^2(\mu\sqrt{n+1})p(n)\right] + \kappa\left[(n+1)p(n+1) - np(n)\right] \\
& + r\lambda\Big\{ \left[(n+1)\sin^2(\mu\sqrt{n+1})p(n) - n\sin^2(\mu\sqrt{n})p(n-1)\right] \\
& + n_b\left[n\sin^2(\mu\sqrt{n-1})p(n-2) - (n+1)\sin^2(\mu\sqrt{n})p(n-1)\right]\Big\} \\
& + r\frac{\lambda^2}{2}\Big\{ (n+2)(n+1)\sin^2(\mu\sqrt{n+2})p(n+1) - (n+1)(2n+1)\sin^2(\mu\sqrt{n+1})p(n) + n^2\sin^2(\mu\sqrt{n})p(n-1) \\
& + n_b^2\left[n(n-1)\sin^2(\mu\sqrt{n-2})p(n-3) - n(2n+1)\sin^2(\mu\sqrt{n-1})p(n-2) + (n+1)^2\sin^2(\mu\sqrt{n})p(n-1)\right]\Big\}.
\end{aligned} \tag{8.1}$$

At steady state, we can get a recursion relation for the photon number.

$$p(n+1) = \frac{r\Lambda_2(n)\sin^2\left(g\tau\sqrt{n+1}\right) + \kappa n_b(n+1)}{r\Lambda_1(n)\sin^2\left(g\tau\sqrt{n+2}\right) + \kappa(1+n_b)(n+1)} \times p(n) = q(n)p(n), \tag{8.2}$$

where

$$\Lambda_2(n) = 1 - \lambda(n+1) + \frac{\lambda^2}{2}\left[(n+1)^2 - n_b^2(n+3)(n+2)\right], \tag{8.3}$$

$$\Lambda_1(n) = \frac{\lambda^2}{2}(n+2)(n+1) + n_b\lambda(n+3)\left(1 - n_b\frac{\lambda}{2}(n+3)\right). \tag{8.4}$$

This equation can be used to calculate the exact photon-number distribution and from it all the necessary moments.

Note that this is a valid recursion relation even without damping ($\kappa = 0$). If the feedback strength is set to zero, we get the standard micromaser recursion relation given by Fillipowicz *et al.* [5].

By letting the recursion ratio $q(n)$ equal 1, it can be shown that in the undamped case at large photon numbers for which $\sin^2(\mu\sqrt{n+1}) \approx \sin^2(\mu\sqrt{n+2})$, the mean photon number is approximately $1/\lambda$. This is quite different from the standard case where the mean photon number is strongly dependent on the ratio r/κ which is known in the literature as N_{ex}.

IX. THE EFFECT OF FEEDBACK

In this section, we present the results of numerical solutions of the recursion relation (8.2). We calculate the probability distribution and thus the mean and normalized standard deviation of the photon number. The normalized standard deviation is defined in relation to the standard deviation of a Poissonian $\sigma_p = \sqrt{\bar{n}}$ in the following way:

$$\sigma = \sqrt{\frac{\langle n^2\rangle - \langle n\rangle^2}{\bar{n}}}\,, \tag{9.1}$$

hence, if the distribution has the same variance as a Poissonian of the same mean the normalized standard deviation σ will be 1. Values less than 1 indicate sub-Poissonian statistics.

We present results for various values of the feedback parameter λ and for different amounts of damping κ. The best results occur for the zero damping case where negligible standard deviations can be achieved.

A. Significant damping $\kappa = 1$ N_{ex}=100

Here, we set the pumping rate to be 100 atoms per second and a damping coefficient of 1. That corresponds to a mean cavity photon lifetime of 1 sec. In Figs. 2(a) and 2(b), respectively, we present the mean and normalized standard deviation of the micromaser with no feedback. These are simply the well known standard results for the micromaser. We see that the maximum possible photon number is approximately 100, which is equal to the mean number of atoms passing through the cavity in one cavity lifetime N_{ex}. We can also see that the standard deviation reaches very low values on the order of 0.35. The periodicity in the behavior of the micromaser is due to the second order phase transitions [5], where the photon-number distribution passes through a multiple peaked stage. At these points the standard deviation in the distribution becomes super-Poissonian.

Figures 3(a) and 3(b) show the effects of a small amount of feedback $\lambda = 0.02$. This corresponds to 4% feedback due to our definition of the feedback superoperator without the factor of 2 used in the normal damping super operator. We see that the feedback has quite a drastic effect on the photon number. The maximum mean photon number drops down to roughly 30. The more interesting effect is seen in the standard deviation plot [Fig. 3(b)], where we see that the peaks in the standard deviation are reduced while the troughs are increased. The feedback thus seems to degrade already sub-Poissonian states of the field in certain regions but improves the super-Poissonian ones. The position of the transition from one photon-number branch to another is also affected by the feedback. The location of these transitions moves out to larger values of λ, which is simply a result of the reduction in mean photon number requiring a larger value of the pumping μ.

We have found that in this large damping regime, the feedback has a similar effect to the introduction of some of the atoms in the ground state. This appears to be reasonable if one looks at the recursion relation for the micromaser with no feedback and the relative fractions of atoms in the upper and lower states given by λ_2 and λ_1, respectively. The recursion relation is then

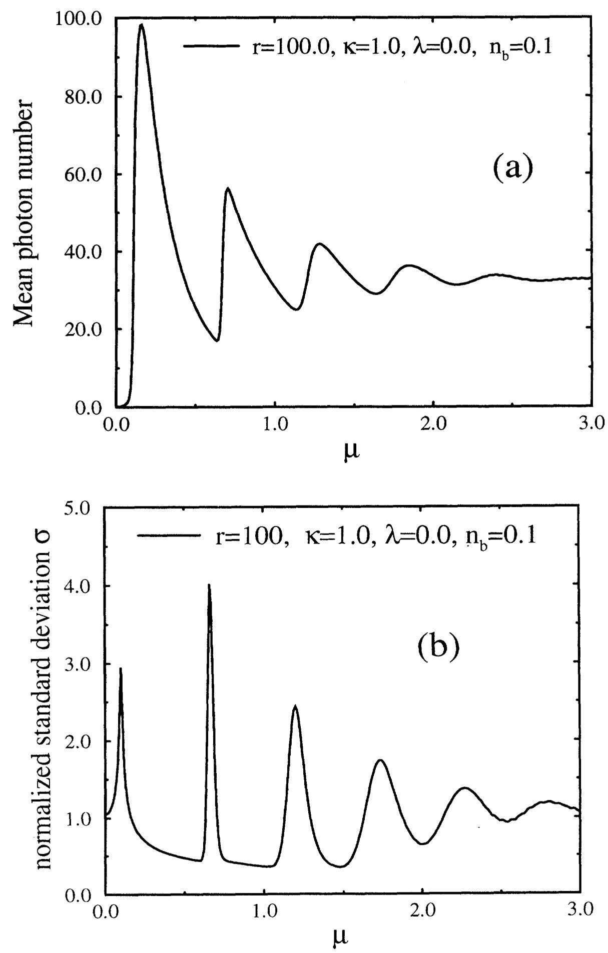

FIG. 2. The mean photon number (a), and normalized standard deviation (b), for the micromaser without feedback. Here, $r = 100$, $\kappa = 1$, $n_b = 0.1$.

$$p(n+1) = \frac{r\lambda_2 \sin^2(\mu\sqrt{n+1}) + \kappa n_b(n+1)}{r\lambda_1 \sin^2(\mu\sqrt{n+1}) + \kappa(1+n_b)(n+1)} p(n). \tag{9.2}$$

Comparing this with the feedback recursion relation (8.2) we see that both have a $\sin^2$ term in the denominator. However, in the limit of small damping, we can see that these relations become quite different. Whereas for the feedback case, we have an n dependent recursion relation, in the standard case we simply get

$$p(n+1) = \frac{\lambda_2}{\lambda_1} p(n). \tag{9.3}$$

This only gives a normalizable distribution in the trivial case of $\lambda_1 > \lambda_2$. In the feedback case, we can get nontrivial distributions. As the damping becomes larger, the $\sin^2$ term in the denominator becomes less significant and the behavior of the two cases becomes similar. Figures 4(a) and 4(b) show a comparison of the mean photon number and standard deviation for the two cases, for $r = 100$ and $\kappa = 1$. We see that for feedback values of $\lambda = 0.005$ and $\lambda = 0.01$, the micromaser behaves in a qualitatively similar manner to cases where we chose 10% and 20% of the atoms to be in the ground state for Figs. 4(a) and 4(b), respectively. This similarity in behavior is reasonable, in general, if one considers the fact that the probability for a ground state atom to make a transition to the excited state by the absorption of a photon is

$$P_e = \left\langle \sin^2(\mu\sqrt{a^\dagger a}) \right\rangle, \tag{9.4}$$

which is quite similar to the emission of a photon and the transition of an excited atom into the ground state [see Eq. (5.2)], which determines the detection current and is, therefore, related to the probability of the absorption of a photon due to the feedback. Thus, there is a direct relationship between the two cases. In fact, one can think of the action of the ground state atoms as a sort of internal feedback mechanism. For larger proportions of atoms arriving in the ground state, the behavior of the micromaser in the two cases becomes different.

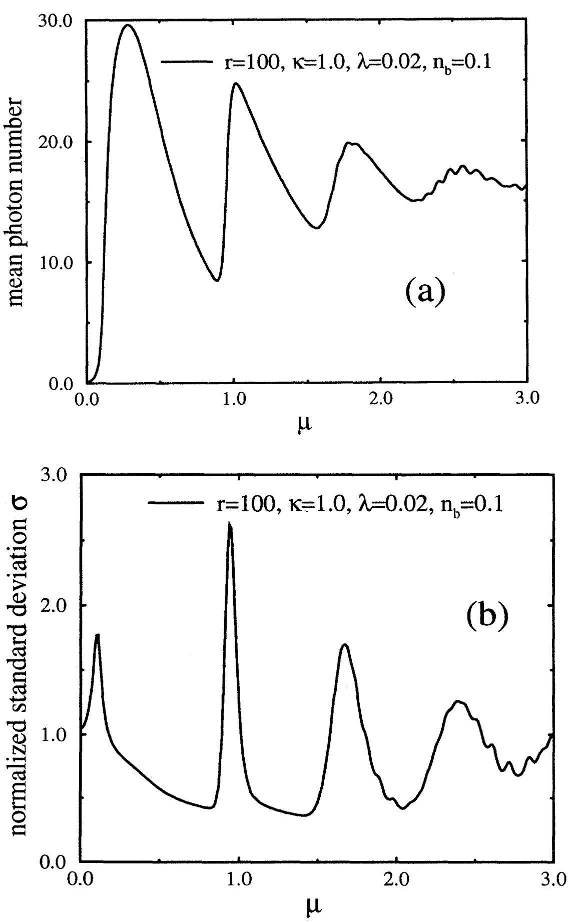

FIG. 3. A plot of mean photon number (a), and the normalized standard deviation (b), with feedback; $\lambda = 0.02$. Here, $r = 100$, $\kappa = 1$, $n_b = 0.1$.

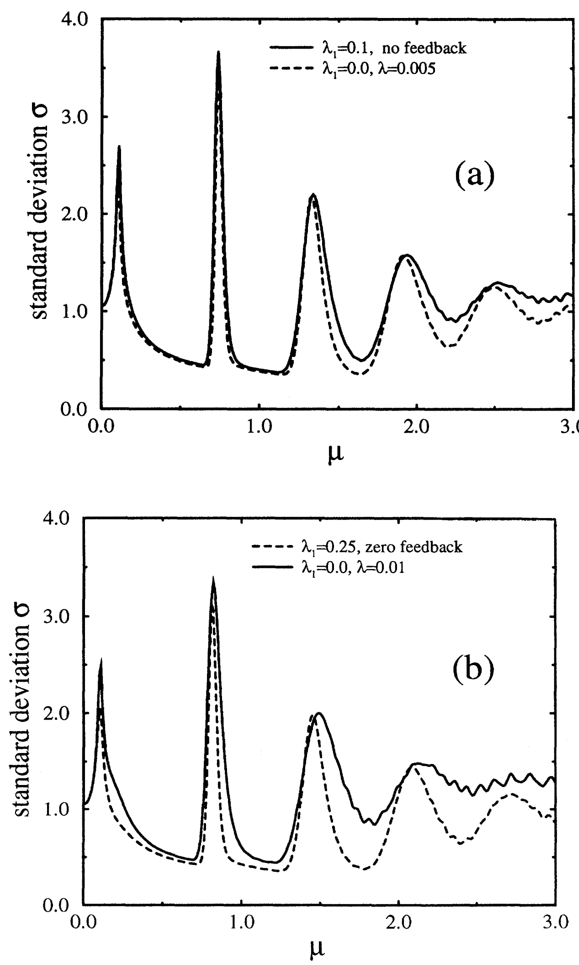

FIG. 4. A comparison of the feedback with the effect of injecting some atoms in the ground state. The fraction of atoms entering in the ground state is (a) $\lambda_1 = 0.1$ and (b) $\lambda_1 = 0.2$. Here, $r = 100$, $\kappa = 1$, $n_b = 0.1$.

B. Small damping

We now reduce the damping significantly and observe what happens to the photon statistics. First, we set the linear damping coefficient κ to be 0.01. This is shown in Figs. 5(a)–5(c). Naively, one would expect the photon number to increase dramatically as in this case the value of N_{ex} is 10 000. However, we actually observe only a slight increase in the photon number and a reduction in the variation in the mean photon number as a function of the pumping. This is a product of the feedback taking over from the linear damping in the role of maintaining the steady state. Since the feedback can keep up with variations in the photon number the resulting steady-state photon number should be much less sensitive to variations in parameters. We can see that the photon-number standard deviation is substantially reduced and we begin to see the formation of the $\bar{n}/2$ plateau for small μ as predicted by the simple amplifier theory. This corresponds to a σ of $\sqrt{2} \approx 0.71$. The structure of the curves

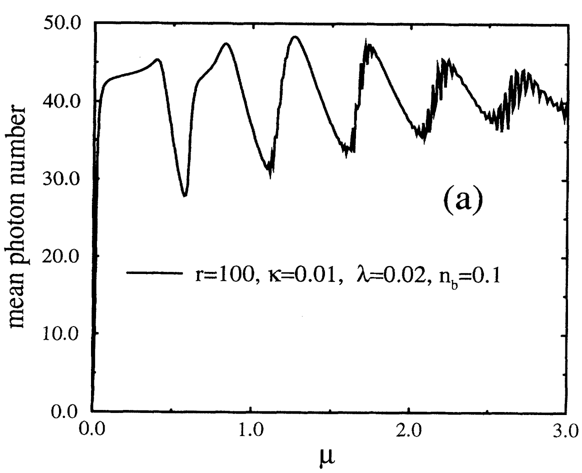

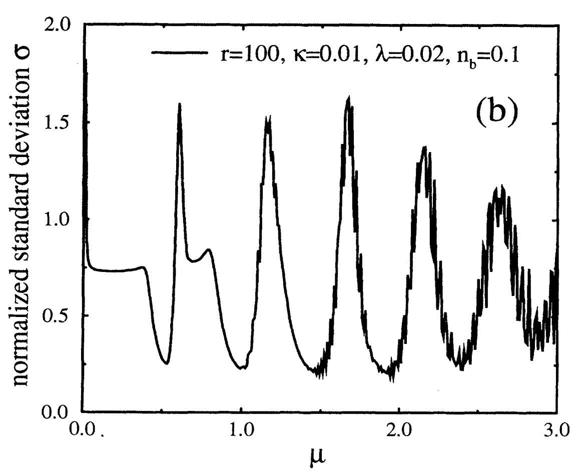

FIG. 5. The effect of feedback in the presence of small damping; $\kappa = 0.01$, $\lambda = 0.02$, $n_b = 0.1$. (a) Mean photon number, (b) normalized standard deviation. Here, $r = 100$, $\kappa = 1$, $n_b = 0.1$.

can be seen to become more irregular at larger μ than previously. This is due to the smoothing effects of the second term in the numerator in Eq. (8.2) being reduced by the lower overall strength of the linear damping κ.

We see the periodic structure begin to move back in with respect to the pumping μ. The position of the minima is now mostly determined by the trapping state condition for the mean photon number $1/\lambda$. The location of these dips approximately satisfies the trapping state condition.

We now reduce the linear damping to zero and again note that under these conditions the micromaser can still reach steady state due to the action of the feedback. This case is shown in Figs. 6(a)–6(c). In this case, the steady-state photon number is constant for small μ. Its value is a little less than $1/\lambda = 50$ because the nonzero temperature of the bath enhances the damping produced by the feedback and reduces the steady state. For larger values of μ, we see the photon number beginning to vary with μ. Around the trapping states the photon number is decreasing. In the standard deviation plot, we see that these states show up as region of greatly reduced σ. It appears that there is some region around the correct value of μ, where the feedback locks the micromaser onto the trapping state. In this region the photon number decreases to compensate for increasing μ. Thus, we can derive an equation for the mean photon number in this region. The trapping state condition for a number state is simply

$$\mu\sqrt{n+1} = m\pi, \tag{9.5}$$

where n is the number of the state and m is an integer corresponding to the order of the dip in the standard deviation. Then the curves in the $n - \mu$ plane are given by

$$n = \frac{(m\pi)^2}{\mu^2} - 1. \tag{9.6}$$

These curves are displayed in dashed lines on the same plot [Fig. 6(a)]. The agreement can be seen to be good for smaller values of μ and deviates slightly for higher values. Overall the agreement is good and supports our claim that the micromaser is locked on to a trapping state. A plot of the probability distribution is shown in Fig. 6(c), where darker colors indicate higher probability. Here, we used the logarithm of the intensity because the distribution was so strongly peaked around the trapping states that normal scale would make most of the information invisible. Here, we can see that the micromaser is essentially close to a trapping state most of the time. In places, however, the wings of the distribution grow significantly and wash out the information when the moments are calculated.

It is important to point out that the high degree of irregularity in the plots is not due to lack of numerical accuracy but a real characteristic of the system.

C. Large photon number

If the feedback is decreased to a smaller value such as 0.002 then the photon number of the micromaser moves to about 500. This can be seen in Figs. 7(a)–7(c). The general features of the behavior are similar to the larger λ case. The interesting feature in this case is the appearance of flat regions in the photon number between the trapping states. These regions correspond to broad distributions with variance $\bar{n}/2$. This is manifested in the standard deviation plot [Fig. 7(b)], as approximately flat regions with a value of about $1/\sqrt{2}$. The structure of the distributions [Fig. 7(c)] and their moments is also much smoother in the smaller feedback case for the same order

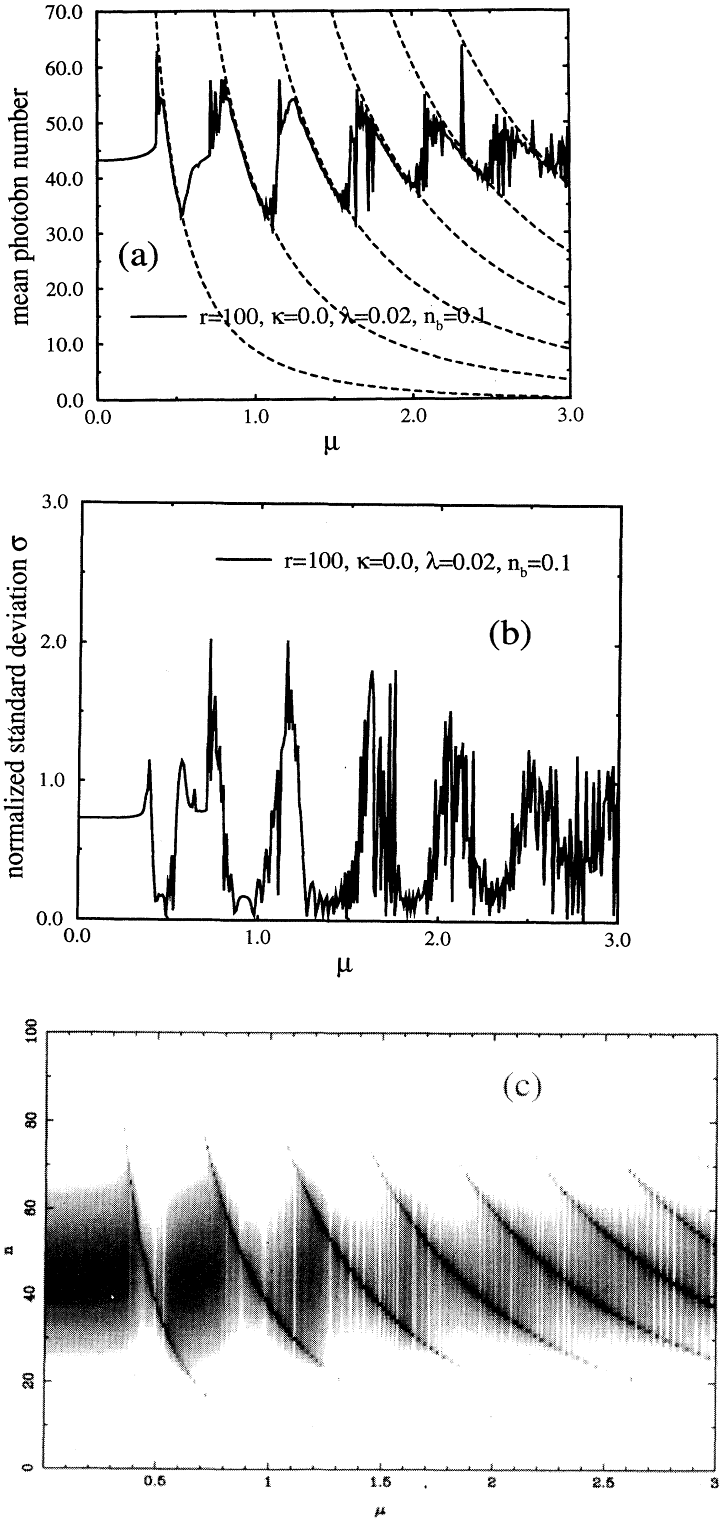

FIG. 6. Feedback with no linear damping at all. The feedback strength is $\lambda = 0.02$ and $n_b = 0.1$. (a) The mean photon number with the curves describing the trapping states, (b) the normalized standard deviation, and (c) the logarithmic photon-number distribution with darker shades corresponding to higher probability. Here, $r = 100$, $\kappa = 0$, and $n_b = 0.1$.

of trapping state. Overall, however, the regularity of the structure seems to depend only on the value of μ. We can see this in Figs. 7(d) and 7(e) which show the moments for μ between 1.0 and 3.0. We see that the irregularity sets in for approximately the same values of μ. It is not clear how the onset of the irregularity can be determined.

D. Quantum island states

A recent paper by Bogar *et al.* [19], presented a study of the micromaser statistics for regions of large μ which were not previously looked at. They found regions where the photon number probability becomes well localized again

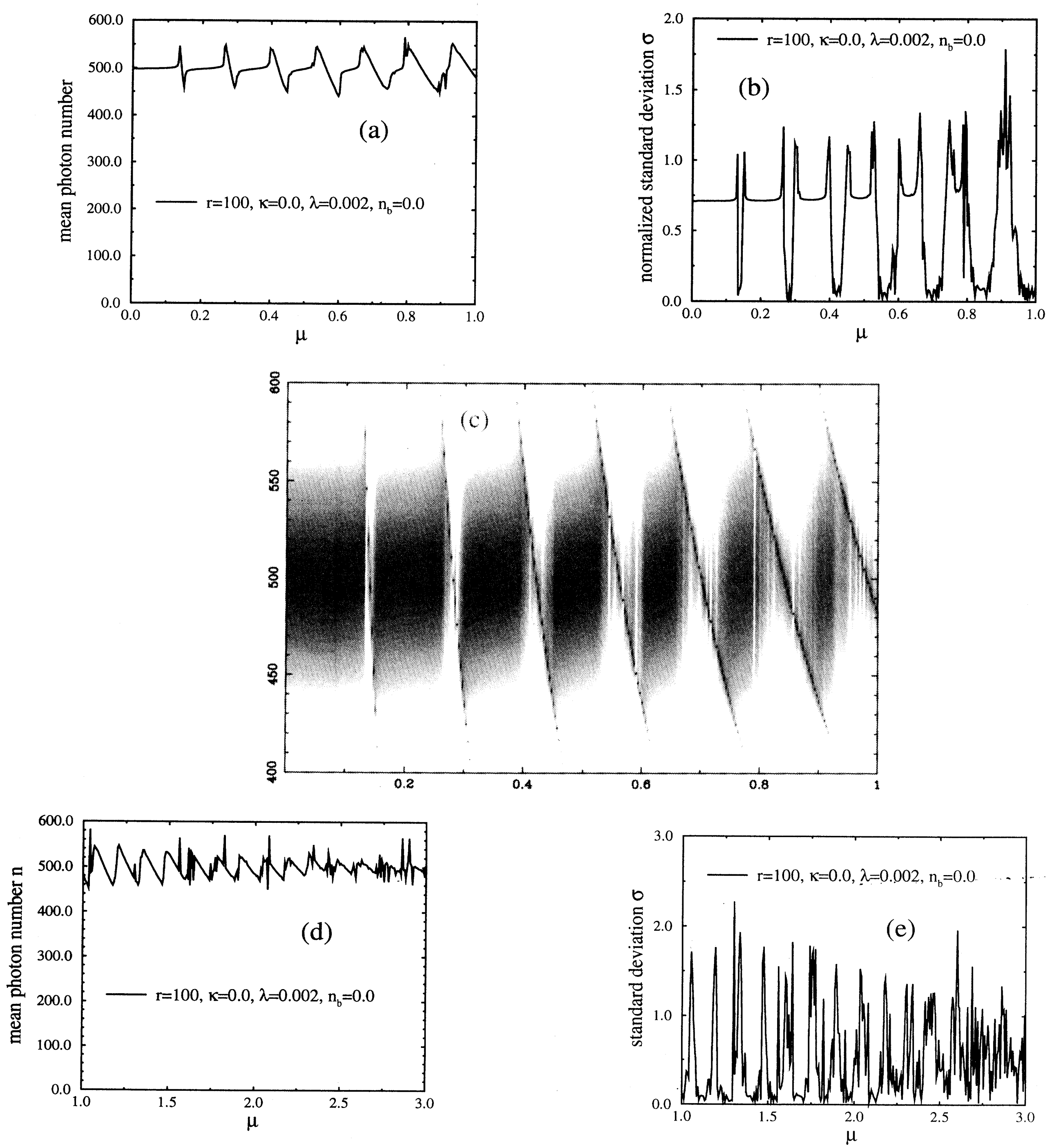

FIG. 7. Small feedback of $\lambda = 0.002$ corresponding to a mean photon number centered about 500. (a) The mean photon number, (b) the normalized standard deviation, and (c) the logarithmic photon-number distribution with darker shades corresponding to higher probability. Here, $r = 100$, $\kappa = 0$, $n_b = 0.0$, and μ is varied from 0 to 1. Also, (d) the mean photon number and standard deviation (e) from $\mu = 1$ to 3.

after initially dispersing. These regions appeared as islands in the two dimensional θ-n space, where $\theta = \sqrt{N_{ex}}\mu$ is the scaled pumping parameter and n is the photon number. It was found that some of these states were strongly sub-Poissonian. There was also a large proportion of these "quantum island states," which were not sub-Poissonian but when some of the atoms were injected in the ground state these states became very sub-Poissonian. We found that if feedback is applied in the same region, these states also become very sub-Poissonian with $\sigma < 0.5$, which corresponds to a noise reduction of at least 75%.

Figure 8(a) shows the dependence of the photon-number distribution normalized standard deviation σ for the quantum island states without the presence of feedback. The peaks in the standard deviation of the normal case correspond to the island states. The roughly flat regions correspond to regimes where the photon-number

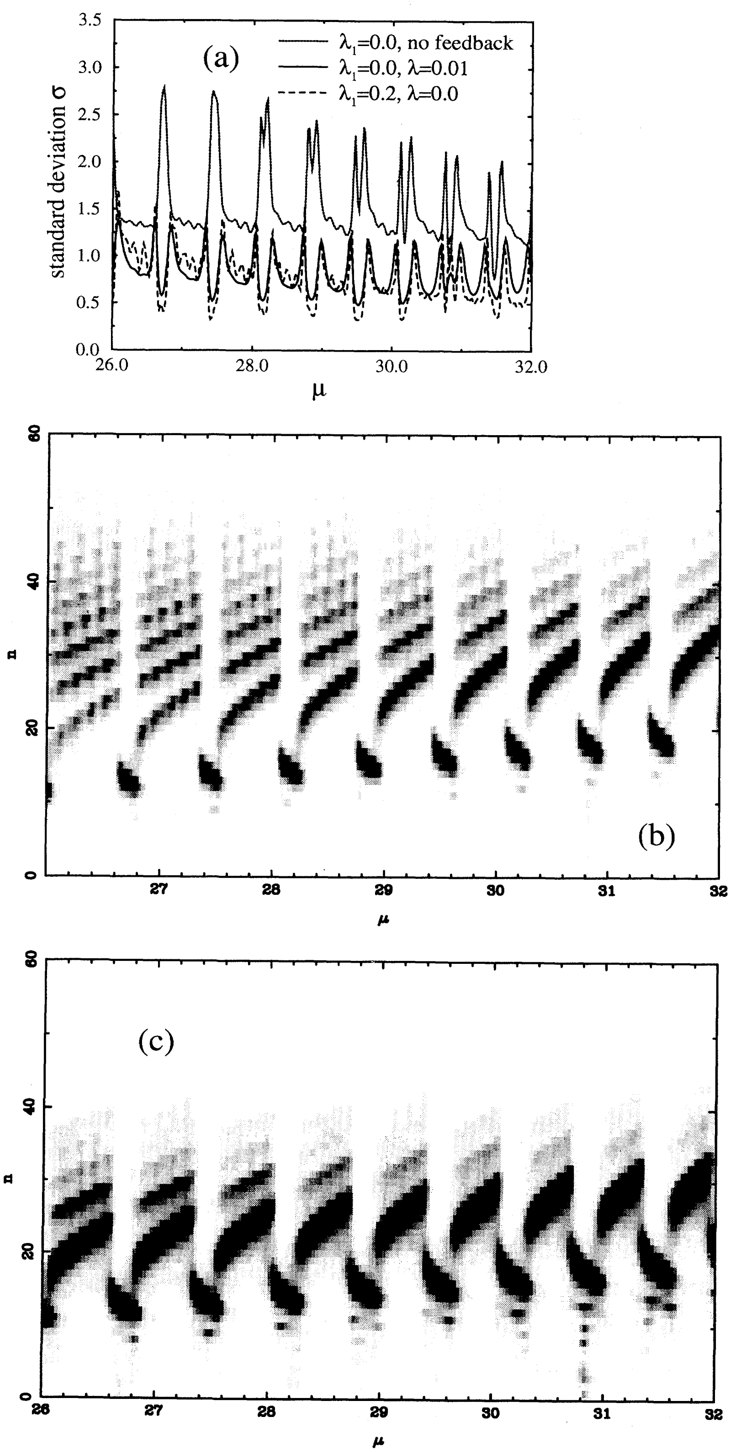

FIG. 8. The effect of feedback on quantum island states. (a) The normalized standard deviation where the solid line is the feedback result and the dashed result is with 20% of the atoms entering in the ground state. The dotted line describes the unmodified behavior ($\lambda_1 = 0.0, \lambda = 0.0$). (b) and (c) show the photon-number distribution for the unmodified and feedback; ($\lambda = 0.01$) cases, respectively. Here, $r = 100$, $\kappa = 1$, and $n_b = 0.1$.

distribution is multipeaked. When the feedback is applied (dashed line), we see that dips form in both types of regions. Surprisingly, the larger dips form at the locations of the island states. That is to say, sub-Poissonian regions develop in both areas but the QIS's form the less noisy ones. This is very similar to the behavior of the micromaser when some of the atoms are injected in the lower state as in the case considered by Bogar *et al.* This is to be expected as we mentioned before, since for significant damping the recursion relation is similar to the recursion relation for the regular micromaser [see Eq. (9.2)]. The dotted line shows the same region in μ but with no feedback and with 10% of the atoms injected in the ground state. We can see that the two methods yield similar results.

The μ-n plot for the probability distribution with no feedback is shown in Fig. 8(b), where $r = 100, \kappa = 1, n_b = 0.1$. This is exactly the case presented in the paper by Bogar *et al.* [19]. We can see the ridges in between the islands as well as the island states themselves. Figure 8(c) shows the probability distribution with the feedback switched on ($\lambda = 0.01$).

X. STOCHASTIC SIMULATIONS

In experiments, one needs some way of confirming that the system is in a nonclassical state. Since it is difficult to detect the light from the micromaser cavity, we need to look at some property of the atoms leaving the cavity. We decided to look at the statistics of the ground state atoms leaving the cavity. This is best done by simulating the system and calculating the detection current. For this purpose we turn, once again, to the quantum-trajectories method. Similar calculation were performed on the standard micromaser by Cresser and Pickles [20]. In this Monte Carlo simulation method, we start with the density matrix or state vector for the system and calculate the probability that a quantum jump [defined in Eq. (6.1)], occurs in a small time interval Δt. The interval should be small enough so that the probability of more than one jump occurring in that time interval is negligible. We then pick a random number and compare it with the probability of the jump. If the random number is less than that probability then the jump has occurred and we apply the appropriate jump superoperator to the system. If there was no jump, we apply the smooth evolution operator. This would include the Hamiltonian evolution and the Liouivillian decay part of the master equation. Strictly speaking this operator should also be applied after the jump. However, the change in the system due to this is negligible compared with the change due to the jump and can be ignored.

Since the master equation for the micromaser conserves the diagonality of the density matrix, we can perform this calculation quite simply assuming the micromaser starts in a thermal state or a number state then for each trajectory, we simply need to keep track of the photon number n. If we find that an atom leaves in the ground state when it entered in the excited state, then we simply increment the photon number by 1. Conversely, if the atom entered in the ground state and left in the excited state, we decrement the photon number by 1. We also perform a test for each time step to see if a photon was absorbed due to the irreversible damping of the field. In this case, the photon number is also decremented. A corresponding procedure is also followed for a thermal photon entering the cavity.

The outline of the calculations at each time step is as follows: First we check to see if an atom has entered the cavity. This is a Poissonian process with an occurrence probability of $r\Delta t$. If an atom enters, then we check whether it is in the excited or ground states. These probabilities are

$$\begin{aligned} &\textbf{Excited-state probability} = \lambda_2 \\ &\textbf{Ground-state probability} = \lambda_1. \end{aligned} \tag{10.1}$$

Depending on the result of this test, we then check whether an emission or an absorption occurred. The emission or absorption probabilities for atoms in the excited and ground states are

$$\begin{aligned} \text{Emission probability} &= \left\langle \sin^2(\mu\sqrt{aa^\dagger}) \right\rangle = \sin^2(\mu\sqrt{n+1}) \\ \text{Absorption probability} &= \left\langle \sin^2(\mu\sqrt{a^\dagger a}) \right\rangle = \sin^2(\mu\sqrt{n}), \end{aligned} \tag{10.2}$$

where n is the photon number. We only need the photon number n to characterize the system since for each trajectory, the system remains in a number state. We then increment or decrement the photon number accordingly. We also need to check whether a photon was lost through damping. This has a probability

$$\kappa\Delta t \left\langle a^\dagger a \right\rangle = \kappa\Delta t n. \tag{10.3}$$

The feedback is performed if the atom was initially in the excited state and left in the ground state. We use a variable $\Delta\kappa$ to hold the amount of excess damping due to feedback. At each time step we calculated the new excess damping by

$$\Delta\kappa \to \Delta\kappa e^{-\beta\Delta t} + \lambda\beta J, \tag{10.4}$$

where J is a variable which is 1 or 0 depending on whether an atom has been detected in the ground state or not, and the exponential is a kind of response or memory function. The parameter β determines how strong the feedback is and for how long it effectively acts in such a way that in the limit as $\beta \to \infty$ the feedback gives a δ-function kick to the damping of the system. The system is Markovian in this limit. A further avenue of investigation is possible here for the study of the non-Markovian behavior of the micromaser.

The idea initially was to calculate the second order correlation function for the ground-state atomic current and to look for antibunching in it. We found, however, that around the trapping states selected by the feedback, the current was so low as to make it impossible to calculate the two-time correlation function due to an insufficiently large sample of atoms. The variance in the arrival distribution of the atoms also provides an experimentally observable signature of the sub-Poissonian nature of the field. However, this variance was also impossible to calculate. We found that the best quantity to look at is the magnitude of the current itself. Consequently, we discovered that over a trapping state region the ground state atomic current becomes very small. The detection current is bounded above by the injection rate of the atoms, that is,

$$I^g_{\mathrm{max}} = r. \tag{10.5}$$

Therefore, when we say that the current was very small, we mean that $I^g \ll r$. This behavior of the current around the trapping state is quite reasonable because at a trapping state the atom undergoes an integral number of transition cycles between the excited and ground states. The probability of leaving in the excited state is therefore close to 1.

Figures 9(a) and 9(b) show a comparison between the analytic result for the photon-number standard deviation σ and the simulated standard deviation and ground state current, respectively. In the first of these figures, we see that the simulated and calculated standard deviations follow each other to a certain degree although the small scale structure is often different. In this calculation, we used quite a large feedback of $\lambda = 0.05$, which corresponds to a mean photon number of about 20. Such a low photon number was required for computational speed reasons, because the system reached steady state after a relatively short period of time. Each point on the curve was calculated with 500 trajectories. This relatively low number was required for the calculation to finish in reasonable time. The incongruities between the results may be due to an inadequate number of trajectories or the system not reaching steady state in the specified time. This is quite likely since near the trapping states very little evolution occurs since most of the time there is no change in the system as the atoms are very likely to leave in the same state they entered in. It is, therefore, possible that a true steady state has not yet been reached. Further numerical work is required in order to clear up this point.

The second figure shows the analytic standard deviation and the steady-state atomic detection current as a function of the pumping μ. We see that the current follows the dips in the standard deviation quite closely. Curiously, the current provides a better indication of the sub-Poissonian nature of the field in the regions where the trapping states occur than if we could observe the standard deviation. It appears that this is the best indicator we can use. It does not seem to be a very good indicator in the region of $\sigma = 1/\sqrt{2}$, where the current varies quite widely. There is a problem for very small μ where the calculated standard deviation differs strongly from the predicted value. This may be due to the system taking longer to reach a steady state because the probability of the emission of a photon is so low.

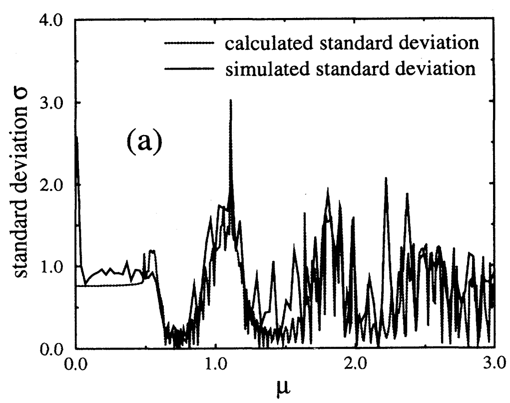

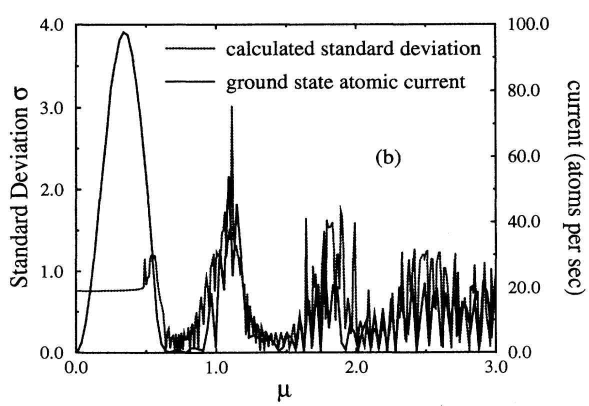

FIG. 9. (a) A comparison of the calculated (dashed line) and simulated (solid line) normalized standard deviations for $\lambda = 0.05$ and $r = 100$, $\kappa = 0$, and $n_b = 0.1$. (b) A comparison of the analytic normalized standard deviation (dashed line), with the ground state steady-state detection current (solid line).

XI. CONCLUSION

In this paper, we presented the properties of the micromaser with electro-optic feedback applied after the detection of an atom leaving the cavity in the ground state. We looked at the case where all the atoms entered in the excited state. In the analytical study of this problem, we applied the quantum theory of feedback developed by Wiseman and Milburn. We found that the feedback had two distinct regions of behavior, the significant damping regime and the negligible damping regime. For significant amounts of cavity damping, we found that the feedback degraded the sub-Poissonian behavior of the micromaser in the regimes of operation where the micromaser was already sub-Poissonian. However, we also found that it improved the behavior of the micromaser in the super-Poissonian regimes. We also found that in this regime, the feedback produced results which were similar to those produced by injecting a small fraction of the atoms in the lower state. In effect these atoms acted as a sort of intrinsic feedback mechanism.

We also showed that significant noise reduction can be achieved with feedback in the quantum island state regime of the micromaser. Noise suppression of up to 75% was predicted.

In the negligible damping regimes, we found that the feedback strength determines the steady state of the micromaser. The mean photon number was found to be approximately given by the simple relation $\bar{n} = 1/\lambda$. In this regime, the micromaser locks on to the trapping state with approximately $1/\lambda$ photons. We found that these trapping states formed curves in n-μ space, which were given by the trapping condition. There are an infinite number of these trapping condition as the pumping parameter μ is varied.

We also simulated the micromaser using stochastic quantum trajectories and included feedback. We found that the results of the simulations agreed with the general features of the analytical theory but the fine structure in the photon number and standard deviation behavior could not be reproduced. This was conjectured to be due to an insufficient number of trajectories used or the system not yet reaching steady state. This requires investigation.

ACKNOWLEDGMENTS

The authors would like to thank Howard Wiseman, Jim Cresser, and John Slosser for helpful discussions. A.L. would also like to thank the Australian Commonwealth for its support.

[1] G. Rempe, F. Schmidt-Kaler, and H. Walther, Phys. Rev. Lett. **64**, 2783 (1990).
[2] H. Walther, Phys. Rep. **219**, 263 (1992).
[3] P. Meystre, Phys. Rep. **219**, 243 (1992).
[4] H.M. Wiseman, Phys. Rev. A **49**, 2133 (1994).
[5] P. Fillipowicz, J. Javanainen, and P. Meystre, Phys. Rev. A **34**, 3077 (1986).
[6] P. Meystre, Opt. Lett. **12**, 669 (1987); J. Krause, M.O. Scully, and H. Walther, Phys. Rev. A **36**, 4547 (1987).
[7] G.J. Milburn, in *The Quantum Theory of Measurement in Quantum Optics*, Proceedings of the Fifth Physics summer school in Atomic and Molecular Physics and Quantum Optics (World Scientific, Singapore, 1992).
[8] K. Kraus, *States, Effects and Operations: Fundamental Notions of Quantum Theory* (Springer, Berlin, 1983).
[9] E.T. Jaynes and F.W. Cummings, Proc. IEEE **51**, 89 (1963).
[10] G.J. Milburn, Phys. Rev. A **36**, 744 (1987).
[11] H.J. Carmichael, in *An Open Systems Approach to Quantum Optics*, Lecture Notes in Physics (Springer, Berlin, 1993); J. Dalibard, Y. Castin, and K. Molmer, Phys. Rev. Lett. **68**, 580 (1992); P. Zoller, M. Marte, and D.F. Walls, Phys. Rev. A **35** 198 (1987); M.D. Srinivas and E.B. Davies, Opt. Acta **28**, 981 (1981).
[12] H.M. Wiseman and G.J. Milburn, Phys. Rev. Lett. **70**, 548 (1993).
[13] J.D. Cresser, Phys. Rev. A **46**, 5913 (1992).
[14] H.M. Wiseman and G.J. Milburn, Phys. Rev. A **47**, 1652 (1993).
[15] G. Lindblad, Commun. Math. Phys. **48**, 199 (1976).
[16] C.M. Caves and G.J. Milburn, Phys. Rev. A **36**, 5543 (1987).
[17] R. Görtz and D.F. Walls, Z. Phys. B **25**, 423 (1976).
[18] C.W. Gardiner, *Handbook of Stochastic Methods*, edited by H. Haken, Series in Synergetics Vol. 13 (Springer-Verlag, Berlin, 1985).
[19] P. Bogar, J.A. Bergou, and M. Hillary, Phys. Rev. A **50**, 754 (1994).
[20] J.D. Cresser and S.M. Pickles, Phys. Rev. A **50**, 925 (1994).

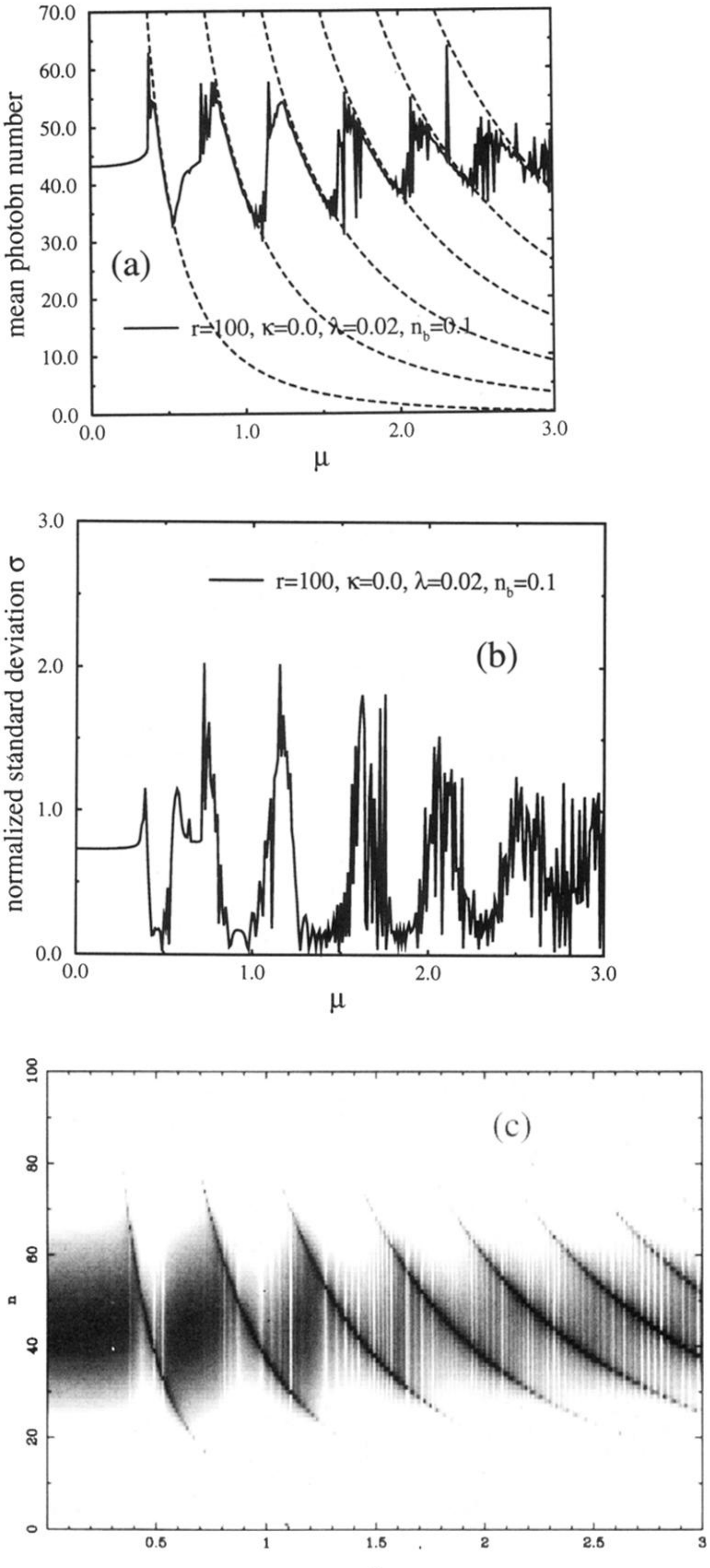

FIG. 6. Feedback with no linear damping at all. The feedback strength is $\lambda = 0.02$ and $n_b = 0.1$. (a) The mean photon number with the curves describing the trapping states, (b) the normalized standard deviation, and (c) the logarithmic photon-number distribution with darker shades corresponding to higher probability. Here, $r = 100$, $\kappa = 0$, and $n_b = 0.1$.

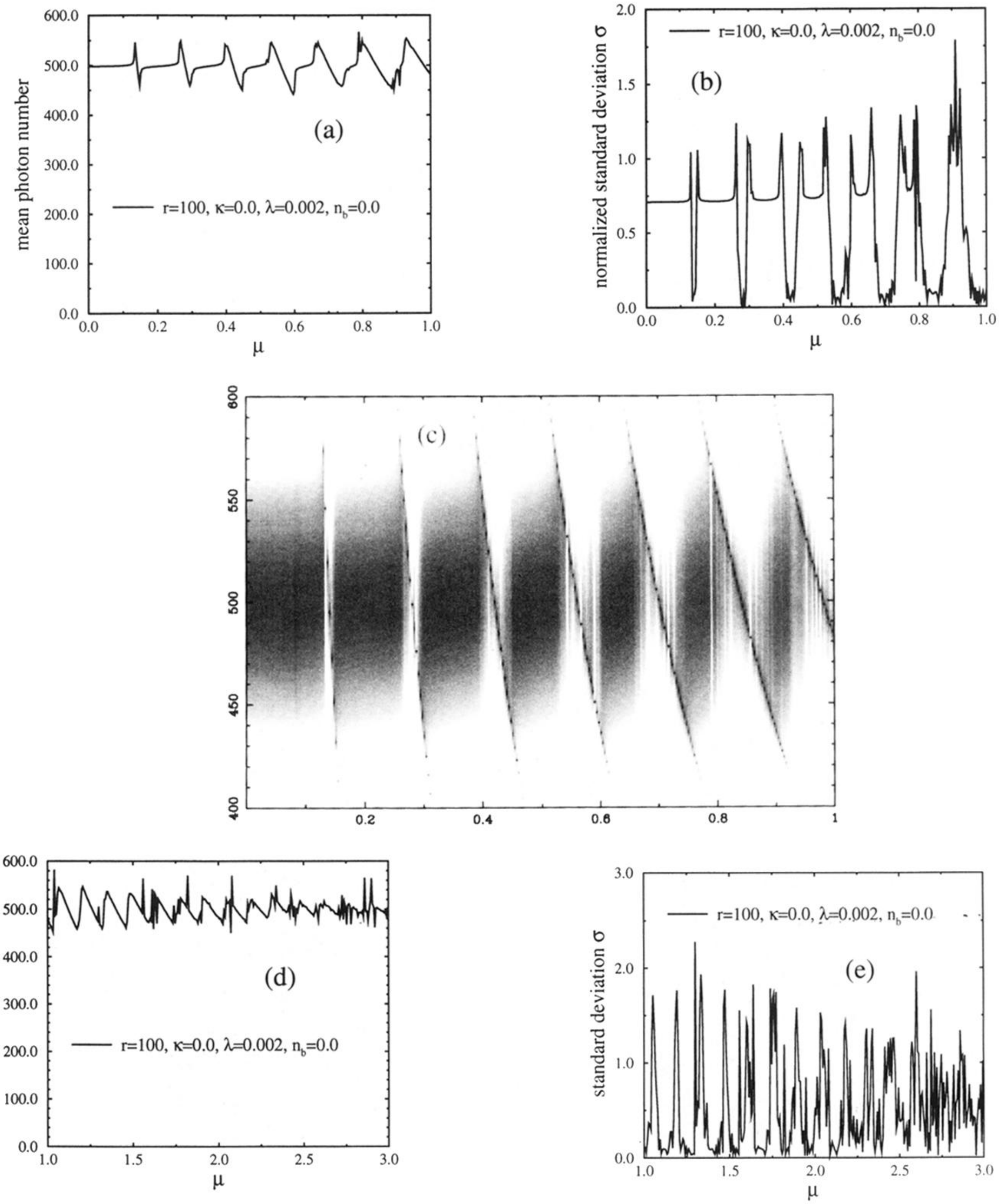

FIG. 7. Small feedback of $\lambda = 0.002$ corresponding to a mean photon number centered about 500. (a) The mean photon number, (b) the normalized standard deviation, and (c) the logarithmic photon-number distribution with darker shades corresponding to higher probability. Here, $r = 100$, $\kappa = 0$, $n_b = 0.0$, and μ is varied from 0 to 1. Also, (d) the mean photon number and standard deviation (e) from $\mu = 1$ to 3.

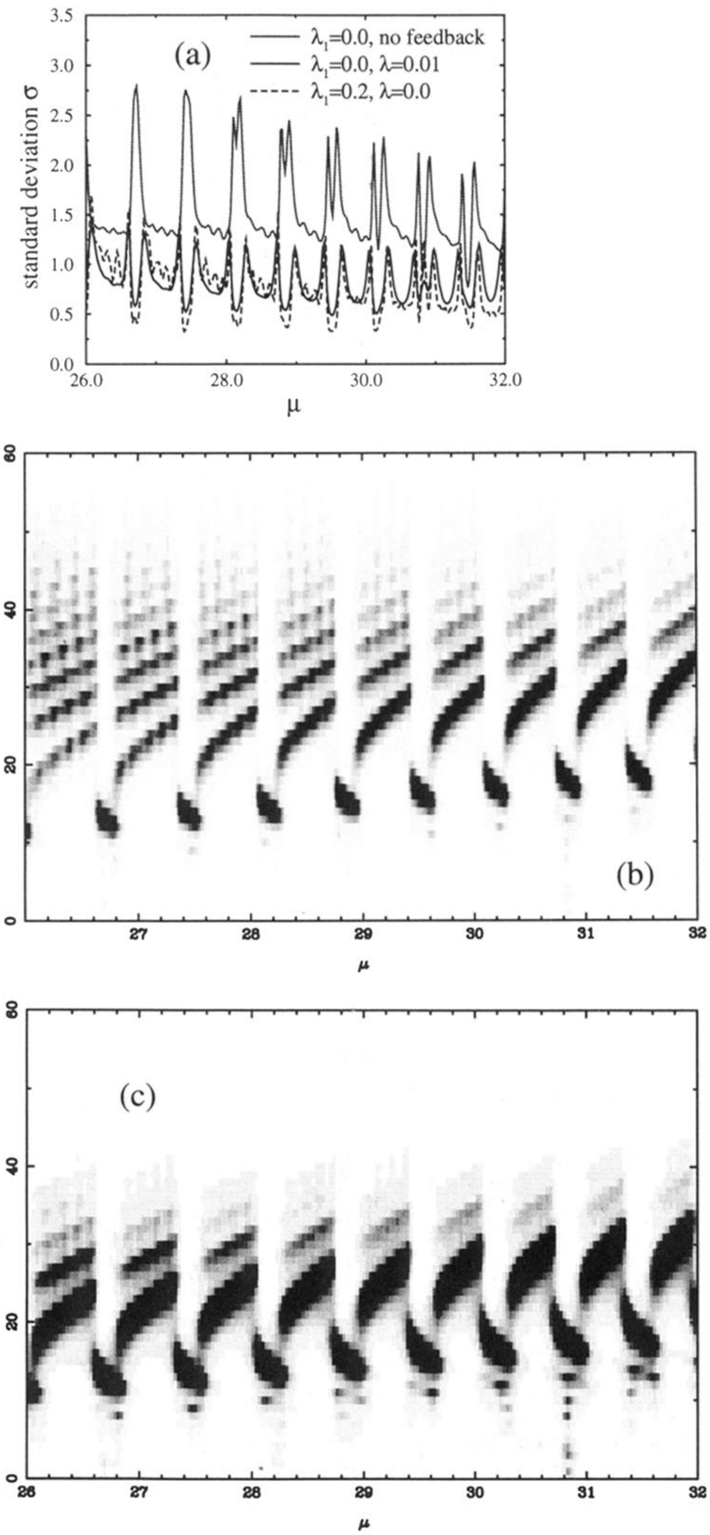

FIG. 8. The effect of feedback on quantum island states. (a) The normalized standard deviation where the solid line is the feedback result and the dashed result is with 20% of the atoms entering in the ground state. The dotted line describes the unmodified behavior ($\lambda_1 = 0.0, \lambda = 0.0$). (b) and (c) show the photon-number distribution for the unmodified and feedback; ($\lambda = 0.01$) cases, respectively. Here, $r = 100$, $\kappa = 1$, and $n_b = 0.1$.